

Transient theory of cavity-modified spontaneous emission

Jonathan Parker and C. R. Stroud, Jr.

The Institute of Optics, The University of Rochester, Rochester, New York 14627

(Received 18 December 1986)

We present a numerical and analytical study of a multimode Jaynes-Cummings model describing the spontaneous decay of a single atom in a high- Q cavity. The theory of cavity-modified spontaneous emission is discussed in terms of quantities that have clear physical interpretations: the photon wave packet radiated by the atom, its reflection by the cavity boundaries, and its reabsorption by the atom. Multimode corrections to the single-mode Jaynes-Cummings model are calculated. The multimode corrections are formulated in terms of quantities that may be calculated by solving the single-mode equations of motion.

I. INTRODUCTION

The problem of an atom interacting with a single mode of the electromagnetic field in a high- Q cavity has been the subject of hundreds of papers since the early investigation by Jaynes and Cummings.¹ Recently, it has been possible to study the theoretical predictions in the laboratory using atoms excited to Rydberg states interacting with microwave fields in superconducting cavities. Both enhanced² and inhibited spontaneous emission³ have been observed.

The single-mode assumption of the conventional Jaynes-Cummings model is an idealization that is useful and reasonably accurate for a wide range of problems. There are, however, many problems for which this assumption is invalid. In the single-mode model there is no retardation. Any changes in the field as the atom radiates and absorbs are instantaneously communicated throughout the cavity. In a real cavity, a spontaneously decaying atom radiates a field which propagates to the cavity walls where it is partly reflected, and partly absorbed. The reflected field then acts back on the atom carrying information about the cavity walls and about the state of the atom itself at earlier times. To study these transients a multimode description of the electromagnetic field is necessary.

In this paper we will investigate the transient interaction of a one-electron atom with its own spontaneously radiated fields in a high- Q cavity. For simplicity it is assumed that the atom is near the center of a spherical microwave cavity. The atom is excited from the ground state to a Rydberg eigenstate with an optical laser pulse of duration short compared to the round trip time of light in the cavity. Our aim is to show how such a model reduces to the single-mode Jaynes-Cummings model in the proper limit and to examine some of the ways in which the single-mode model fails.

In a number of ways the multimode model clarifies rather than complicates the physics of cavity-modified spontaneous emission. For example, the Rabi frequency of the two-level atom and similarly the amplitude of the Rabi oscillations depend very sensitively on whether or not the atom is resonance with a cavity mode. The fre-

quency of the cavity mode depends in turn on the boundary conditions, and on the size and shape of the cavity. The atom, in order to undergo Rabi oscillations of the proper frequency and amplitude must somehow acquire information about the boundaries of the cavity. The picture that emerges from our discussion is that the atom learns of the boundary conditions by interrogating the boundary with its radiated photon wave packet.

The success of recent experimental work has stimulated theoretical work in both the single-mode and multimode models. To give just a few recent examples, there have been investigations of the quantum statistics of single-atom radiation in damped cavities,⁴ cavity-modified Lamb shifts,⁵ and absorption spectra.⁶ In a related set of experiments Dehmelt and co-workers have developed methods to trap single electrons or ions in cyclotron orbits similar to the circular orbit Rydberg states. Experiments have included the successful demonstration of cavity-inhibited spontaneous radiation,⁷ and high-precision measurements of the electron's magnetic moment. The high-precision experiments have made necessary careful theoretical study of the influence of the cavity on the orbital energy of the trapped ion.⁸

Our discussion begins in Sec. II with a review of Heisenberg-picture quantum electrodynamical equations that describe spontaneous emission in free space. We develop a model cavity and modify the equations of motion to describe the effect of a spherical cavity. In Sec. III numerical solutions of the cavity-modified equations are discussed. In Sec. IV simple physical explanations of the numerical results are given. In Sec. V it is shown that the multimode Heisenberg equations, in a certain limit, are formally identical to the single-mode equations. In Sec. VI it is shown that the analysis of Secs. I–V is applicable in principle to a Rydberg atom experiment. In Sec. VII some of the ways in which the single-mode model fails are discussed, and a scheme for calculating multimode corrections to the single-mode model is presented.

II. CAVITY-MODIFIED SPONTANEOUS EMISSION

The quantity of primary interest to us is the rate of change of the atomic Hamiltonian \hat{H}_a . When we special-

ize to a two-level atom, the atomic Hamiltonian will be proportional to the excited-state population of the atom. In the presence of the vector potential $\hat{\mathbf{A}}(t)$, the Heisenberg equation of motion is

$$\begin{aligned} \frac{d}{dt}\hat{H}_a &= \frac{e}{mc} \left[\frac{d}{dt}\hat{\mathbf{p}} \right] \cdot \hat{\mathbf{A}}^{(+)}(0,t) \\ &+ \frac{e}{mc} \hat{\mathbf{A}}^{(-)}(0,t) \cdot \left[\frac{d}{dt}\hat{\mathbf{p}} \right], \end{aligned} \quad (1)$$

where $\hat{\mathbf{p}}$ is the canonical momentum operator, and the carets on top of the variables imply that the variables are

$$\hat{\mathbf{A}}^{(+)}(0,t) = -\frac{2e}{3\pi mc^2} \frac{d}{dt} \int_0^{\omega_c} d\omega \exp(-i\omega t) \int_{-\infty}^{\infty} dt' \mathcal{R}(t,t') \hat{\Pi}(t') \exp(i\omega t'), \quad (2)$$

where the rectangular function $\mathcal{R}(t,t')$ is unity for $0 < t' < t$, $\frac{1}{2}$ at $t'=0$ and $t'=t$, and 0 elsewhere. The kinetic momentum operator of the atom $\hat{\mathbf{p}} - e\hat{\mathbf{A}}/c$, is denoted $\hat{\Pi}$, and ω_c is a frequency cutoff. In deriving (2) we have discarded time-dependent terms of the sort $\hat{a}_k(0)\exp(-i\omega_k t)$, where $\hat{a}_k(0)$ is the $t=0$ photon annihilation operator. Terms of this sort cannot in general be discarded, but they play no role in the discussion that follows and henceforth will be neglected. Throughout this paper, except where otherwise noted, it is assumed that the initial state of the system is $|e\rangle$, which signifies that the atom is in the excited state, and the field in the vacuum state.

To show how this formalism may be used to describe spontaneous emission, we apply it to the decay of an atom in free space. The first step is to evaluate the field $\hat{\mathbf{A}}^{(+)}(0,t)$. Equation (2) resembles a Fourier transform of an inverse Fourier transform but with complications. It follows from Eq. (A7) that

$$\begin{aligned} \hat{\mathbf{A}}^{(+)}(0,t) &= -\frac{2e}{3mc^2} \frac{d}{dt} \hat{\mathbf{p}}^{(+)} \\ &- \left[\frac{2e}{3mc^2} \right]^2 \frac{e}{c} \frac{d^2}{dt^2} \hat{\mathbf{p}}^{(+)} + \dots \end{aligned} \quad (3)$$

To get $\hat{\mathbf{p}}^{(+)}$, the terms in the Fourier expansion of $\hat{\mathbf{p}}$ that go as $\exp(+i|\omega|t)$ are thrown away. This is how we will define the positive frequency parts of atomic operators. For optical transitions in free space, each succeeding term in (4) is of order α^3 smaller than the previous term. The higher-order terms arise from the $\hat{\mathbf{A}} \cdot \hat{\mathbf{A}}$ part of the interaction Hamiltonian. Substituting (3) into (1) and neglecting higher-order terms yields a formula reminiscent of Larmor's formula for the power radiated by an accelerated charge, $dH_a/dt \propto (d\hat{\mathbf{p}}/dt) \cdot (d\hat{\mathbf{p}}^{(+)}/dt) + \text{H.a.}$

The atomic Heisenberg operators can be written as linear combinations of the transition operators $\hat{\sigma}_{ij}(t)$ (Appendix A). The quantity $d\hat{\mathbf{p}}/dt$ is a special case in which the time derivative of an atomic variable may be written as a sum of transition operators:

operators rather than c numbers. In Appendix A the Heisenberg-picture approach is reviewed. The normal ordering of the equations of motion prevents spontaneous transitions from a ground state to a state of higher energy; $\hat{\mathbf{A}}^{(+)}(0,t)$ is the positive frequency vector potential at the location of the atom ($r=0$). The negative frequency potential $\hat{\mathbf{A}}^{(-)}(0,t)$ is the Hermitian adjoint (H.a.) of $\hat{\mathbf{A}}^{(+)}(0,t)$. We use the $\hat{\mathbf{p}} \cdot \hat{\mathbf{A}}$ interaction and the Coulomb gauge throughout.

In the absence of external fields and boundaries (free-space spontaneous emission) $\hat{\mathbf{A}}^{(+)}(0,t)$ can be written in terms of the atomic kinetic momentum operator:

$$\begin{aligned} \frac{d}{dt}\hat{\mathbf{p}} &= \sum_{i,j} \hat{\sigma}_{ij}(t) \left\langle i \left| \frac{[\mathbf{p}, H]}{i\hbar} \right| j \right\rangle \\ &= \sum_{ij} \hat{\sigma}_{ij}(t) \hat{\mathbf{p}}_{ij} i\omega_{ij}, \end{aligned} \quad (4)$$

where ω_{ij} is the transition frequency between atomic states $|i\rangle$ and $|j\rangle$ and where $\hat{\mathbf{p}}_{ij}$ is the matrix element of $\hbar\nabla/i$ on the same states. The quantity $d\hat{\mathbf{p}}/dt$ is the Coulomb acceleration of the electron, whereas $d^2\hat{\mathbf{r}}/dt^2 = (d\hat{\Pi}/dt)/m$ is the total acceleration. We make the dipole approximation. Throughout this paper, in the calculation of $d\hat{\mathbf{p}}/dt$, we will specialize to a two-level atom only after performing the differentiation.

We now specialize to a two-level atom of resonance frequency ω_a . If the ground-state energy of the atom is set to zero, then $H_a = \hbar\omega_a \hat{\sigma}_{ee}(t)$, where $\hat{\sigma}_{ee}$ is the projection operator onto the atom's excited state. It follows that the expectation value of the atomic Hamiltonian on the initial state $|e\rangle$ is $\hbar\omega_a$ multiplied by the excited-state population of the atom. For a two-level atom decaying spontaneously in free space, (1) becomes

$$\begin{aligned} \frac{d}{dt} \hat{\sigma}_{ee} &= -\frac{A_{eg}}{2} [(\hat{\sigma}_{eg} + \hat{\sigma}_{ge})\hat{\sigma}_{ge} + \hat{\sigma}_{eg}(\hat{\sigma}_{eg} + \hat{\sigma}_{ge})] \\ &= -A_{eg} \hat{\sigma}_{ee}, \end{aligned} \quad (5)$$

where A_{eg} is the Einstein A coefficient.

Equations (2), (3), and (5) are the equations that will be modified in order to study cavity-modified spontaneous emission. Equation (1) is always true, but (2) for $\hat{\mathbf{A}}^{(+)}$ must be modified so that the field satisfies the cavity boundary conditions.

To make the discussion as free from complications as possible, the cavity is chosen to be spherical with the atom placed exactly at the center. The cavity is assumed to be lossless. In Sec. V the model will be generalized to include losses.

The boundary conditions require that the component of the electric field parallel to the surface is zero at the boundary $|\mathbf{r}|=R$. Consequently, the boundary conditions are satisfied if $\hat{\mathbf{A}}(\mathbf{r},t)\cdot\mathbf{u}_\theta=0$, where $\mathbf{u}_\theta=\mathbf{r}\times(\mathbf{r}\times\mathbf{p}_{\text{eg}})$ and

$$\hat{\mathbf{A}}(\mathbf{r},t)\cdot\mathbf{u}_\theta=i\frac{e}{\pi mc^2}\int_{-\infty}^{\infty}d\omega f_\theta(\omega r/c)\omega\exp(-i\omega t)\int_{-\infty}^{\infty}dt'\mathcal{P}(t,t')\hat{\mathbf{\Pi}}(t')\cdot\mathbf{u}_\theta\exp(i\omega t'), \quad (6a)$$

with,

$$f_\theta(\omega r/c)=\frac{\sin(\omega r/c)}{(\omega r/c)}+\frac{\cos(\omega r/c)}{(\omega r/c)^2}-\frac{\sin(\omega r/c)}{(\omega r/c)^3}. \quad (6b)$$

In the Coulomb gauge, $\hat{\mathbf{E}}(0,t)$ is proportional to the time derivative of the vector potential $\hat{\mathbf{A}}(0,t)$. The electric field is evidently a Fourier transform of an inverse Fourier transform (apart from some time derivatives). It can be integrated immediately to give a spatial wave packet whose envelope is the \mathcal{P} function multiplied by $\hat{\mathbf{r}}$ (where $d\hat{\mathbf{r}}/dt=\hat{\mathbf{\Pi}}/m$). Such an equation is formally identical to the familiar dipole radiation formula of classical electrodynamics.⁹ There are, however, singularities at $r=0$ and $r=ct$ that are usually neglected in the dipole radiation formula. The singularities arise from the time differentiation of the \mathcal{P} envelope at its discontinuities and will be of some importance to our discussion in Sec. VII.

The boundary conditions are satisfied if $f_\theta(r\omega/c)$ is zero at the boundary $r=R$. Consequently ω is restricted to a set of discrete frequencies $\omega_1, \omega_2, \dots$ [the zeros of $f_\theta(R\omega/c)$] and the integral over ω in (6a) becomes a sum over cavity modes. For large n , ω_n is approximately $2\pi n/\tau$ where τ is the time it takes light to reach the boundary and return to the atom, $c/(2R)$. The orthonormal cavity-mode functions are

$$\mathbf{g}_n(r,\theta,\Phi)=N_n\frac{\omega_n}{c}\left[\frac{3}{4\pi R}\right]^{1/2}\times\left[\begin{aligned} &\sin(\theta)f_\theta(\omega_n r/c)\frac{\mathbf{u}_\theta}{|\mathbf{u}_\theta|} \\ &+\cos(\theta)f_r(\omega_n r/c)\frac{\mathbf{r}}{|\mathbf{r}|} \end{aligned}\right], \quad (7a)$$

with

$$f_r(\omega r/c)=-2\frac{\cos(\omega r/c)}{(\omega r/c)^2}+2\frac{\sin(\omega r/c)}{(\omega r/c)^3}. \quad (7b)$$

To modify Eq. (2) for $\hat{\mathbf{A}}^{(+)}(0,t)$, the integral over frequencies becomes a discrete sum over frequencies ω_n . This may be verified by taking the limit as \mathbf{r} approaches 0 of the positive frequency part of (6a). However, the proper substitution for $d\omega$ is not immediately clear. We argue (Appendix B) that the proper substitution is $N_n^2 2\pi/\tau$. The normalization factor N_n approaches unity rapidly with n . The first three values of N_n^2 are 1.205, 1.029, and 1.012. Consequently the substitution for $d\omega$ is very nearly $\omega_{n+1}-\omega_n$.

where $\hat{\mathbf{A}}=\hat{\mathbf{A}}^{(+)}+\hat{\mathbf{A}}^{(-)}$. All of the components of $\hat{\mathbf{A}}$ parallel to the surface at R are in the direction \mathbf{u}_θ , just as in classical electrodynamics. In the absence of a cavity the field radiated by the dipole is

In the discussion that follows it will be assumed that the atom's resonance frequency is much greater than ω_1 . In the numerical examples of Sec. III we choose $\omega_a \simeq \omega_{10}$, although the results would be the same with $\omega_a \simeq \omega_5$.

III. NUMERICAL SOLUTIONS

For the purposes of numerical integration, the equations are written in the Schrödinger picture. The numerical solution of the equations of motion is discussed in Appendix B. As we will show, the Schrödinger-picture equations and their solutions closely resemble the equations and solutions of the Heisenberg-picture formalism employed here.

In the set of Figs. 1–4 it is assumed that at $t=0$ the atom is in its excited state $|e\rangle$ at the center of the cavity, and that there is no radiation in the cavity.

In Fig. 1 the normalized probability distribution $P_n(t)$ of photons in the cavity modes at time $t=\tau/4$ is plotted. The quantity P_n equals $|b_n(t)|^2/\sum_m|b_m(t)|^2$. The atom is in resonance with the tenth cavity mode; its transition frequency ω_a equals ω_{10} . From Fig. 1 it may be surmised that field is in a coherent superposition of cavity modes, with most of the photon population in the four modes of frequency nearest to ω_a .

Figure 2(a) shows the expectation value of the spatial distribution of energy in the cavity at $t=\tau/4$. The quantity plotted $r^2\langle e|\hat{\mathbf{E}}^{(-)}(r,t)\cdot\hat{\mathbf{E}}^{(+)}(r,t)|e\rangle$, is proportional to the energy contained within a spherical shell of width dr about r . At $t=\tau/2$ [Fig. 2(b)] the field has reached the cavity walls. At $t=3\tau/4$ [Fig. 2(c)] the leading edge

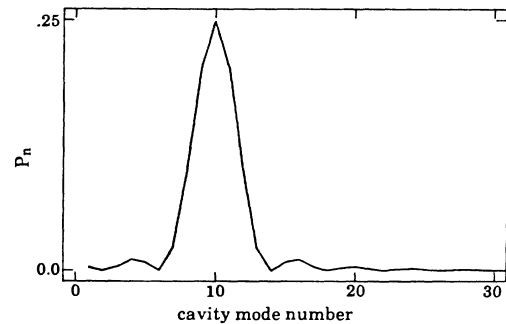


FIG. 1. Normalized probability distribution (P_n) of photons in cavity at $t=\tau/4$. The atom was prepared in the excited state at $t=0$, and $\tau=2R/c$ where R is the cavity radius. The atom is in resonance with the tenth cavity mode.

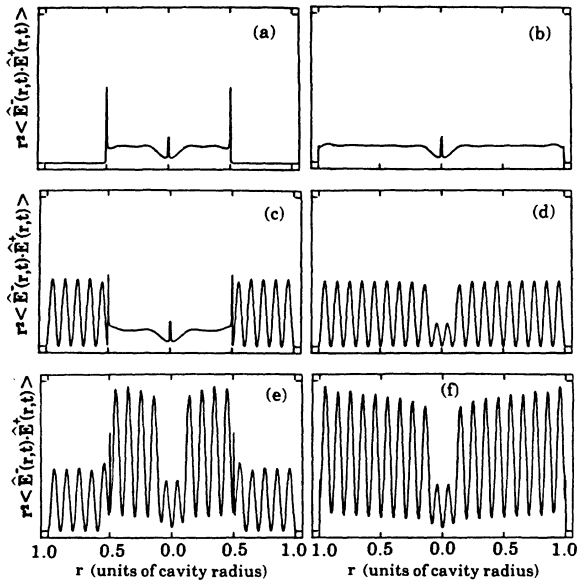


FIG. 2. Expectation value of the spatial distribution of electromagnetic energy in the cavity at various times. The dipole is along the z axis and the field energy density plotted is along the x axis. The atom is in resonance with the tenth cavity mode. (a)–(f) show the field at times $\tau/4$, $\tau/2$, $3\tau/4$, τ , $5\tau/4$, and $6\tau/4$, respectively. The units of the field are arbitrary.

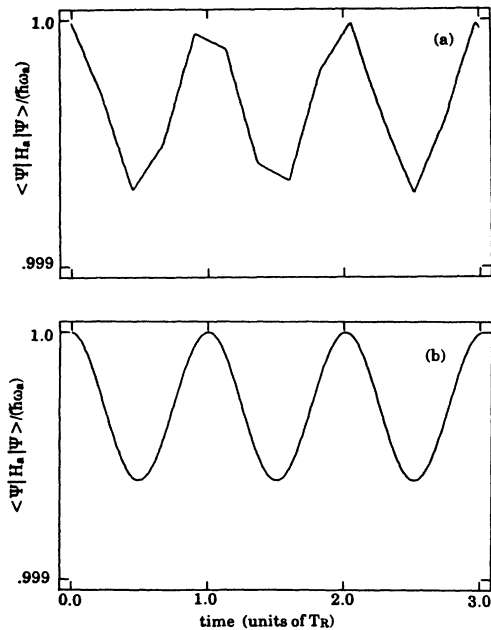


FIG. 3. Expectation value of excited-state population of the atom as a function of time. Time is in units of Rabi period T_R . The atom resonance frequency is detuned from the tenth cavity mode by a frequency Δ , where 4.5Δ equals the frequency separation of cavity modes. (a) is the multimode case. In (b) all modes but the tenth have been discarded.

of the wave packet has begun its return to the atom leaving in its wake what will turn out to be the tenth cavity mode. At $t = \tau$ the leading edge has returned to the atom [Fig. 2(d)] and the field distribution is very nearly that of the tenth cavity mode.

The excited-state population of the atom $\langle e | \hat{H}_a | e \rangle / (\hbar\omega_a)$ is plotted in Fig. 3(a). In Fig. 3 the atom is out of resonance with the cavity, the regime of inhibited spontaneous emission. The atom is detuned from the tenth mode by a frequency $2\pi/(\tau 4.5)$. The detuning Δ is defined $\Delta = \omega_{10} - \omega_a$. In Fig. 3 the atom remains nearly in its excited state and undergoes roughly sinusoidal Rabi oscillations of period $T_R = 4.5\tau$.

At early times $t < \tau$ the atom undergoes Fermi golden rule exponential decay, which appears linear in the figure. The rate of decay is initially the free-space rate, given by the Einstein A coefficient. As the wave packet returns to the atom at $t = \tau$ the excited-state population exhibits a kink, a sudden jump in the rate of decay of the atom, and another is seen at $t = 2\tau$ and at all integer multiples of τ . Figure 3(a) demonstrates that it is the return of the field from the boundaries that modifies exponential decay into sinusoidal Rabi oscillations. There are now 4.5 kinks per Rabi oscillation, indicating that the Rabi frequency very nearly equals the detuning. Figure 3(b) shows the Rabi oscillations in the single-mode Jaynes-Cummings model. All modes but the tenth have been discarded. The approximation is good, but the wave packet interpretation has been lost.

In Fig. 4 the atom is in resonance with the tenth cavity

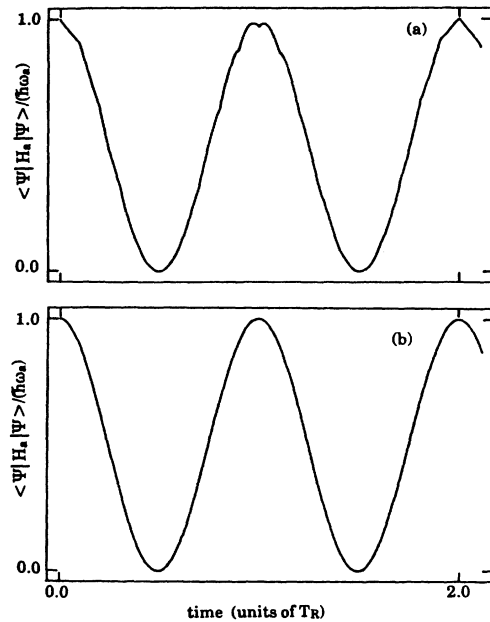


FIG. 4. Expectation value of excited-state population of the atom as a function of time. Time is in units of Rabi period T_R . The atom is in resonance with the tenth cavity mode. (a) is the multimode case. In (b) all modes but the tenth have been discarded.

mode. The dipole moment of the atom has been chosen so that there are exactly ten kinks per Rabi period, $10\tau = T_R$. As the second Rabi oscillation begins at about $t = T_R$, the “angles” of the kinks have changed sign: the rate of change of the expectation value of H_a takes a sudden positive jump at each kink rather than a negative jump as it did at the first few kinks. As t approaches $2T_R$ the kinks return to their initial character suggesting that there is a periodicity of period $2T_R$. This proves to be the case and will be derived analytically in Sec. V. Figure 4(a) is the multimode case, Fig. 4(b) the single-mode case.

IV. WAVE PACKET ANALYSIS OF INHIBITED SPONTANEOUS EMISSION

The Rabi oscillations of Fig. 3(a) can be explained very simply in terms of Eq. (1) for $d\hat{H}_a/dt$ and Eq. (2) for the

$$\hat{\mathbf{A}}^{(+)}(0,t) = -\frac{2e}{3\pi mc^2} \frac{2\pi}{\tau} \frac{d}{dt} \left[\exp(-i\omega_{n_0}t) \int_0^t dt' \exp(i\omega_{n_0}t') (\hat{\mathbf{\Pi}}^{(+)} + \hat{\mathbf{\Pi}}^{(-)}) K(t-t') \right], \quad (8a)$$

with

$$K(t-t') = \sum_{n_0-M}^{n_0+M} N_n^2 \exp[i(\omega_n - \omega_{n_0})(t-t')]. \quad (8b)$$

The Fourier-like kernel $K(t-t')$ is a sum over $2M+1$ modes, which are evenly spaced in frequency to first approximation. It is a series of sharp peaks, each of width about τ/M . It is quasiperiodic with the peaks occurring at intervals of length τ . The peaks are narrow enough to behave as a δ function for the slowly varying part of the integrand $\hat{\mathbf{\Pi}}^{(+)}(t)\exp(i\omega_{n_0}t)$, but not for the rapidly varying part $\hat{\mathbf{\Pi}}^{(-)}(t)\exp(i\omega_{n_0}t)$. The negative frequency parts of $\hat{\mathbf{A}}^{(+)}(0,t)$ then are strongly, but not entirely, suppressed. To good approximation, we may ignore the negative frequency parts, neglect the $\hat{\mathbf{A}}$ in $\hat{\mathbf{\Pi}}$, and apply the time derivative in (8) only to the $\exp(-i\omega_{n_0}t)$ to get

$$\begin{aligned} \hat{\mathbf{A}}^{(+)}(0,t) = & -\frac{2e}{3mc^2} \frac{d}{dt} \hat{\mathbf{p}}^{(+)}(t) \\ & + \frac{4e}{3mc^2} \sum_{m=1}^{[t/\tau]} i\omega_{n_0} \hat{\mathbf{p}}^{(+)}(t-m\tau) \\ & \times \exp(-i\omega_{n_0}m\tau), \quad (9) \end{aligned}$$

where $[t/\tau]$ is the largest integer less than t/τ . The first term in (9) is the radiation-reaction field. The other term is the sum of fields radiated at earlier times returning from the boundaries. The phase factor indicates that the fields do not in general return in phase with the dipole.

In deriving (9) we have assumed that the principal Fourier components of $\hat{\mathbf{\Pi}}$ are near ω_{n_0} and $-\omega_{n_0}$ in frequency, which is true of the zeroth-order solution of $\hat{\mathbf{\Pi}}$ in the case of a two-level atom. The argument generalizes

field at the atom $\hat{\mathbf{A}}^{(+)}(0,t)$.

The first step is to modify (2) by letting the integral over ω become a sum over cavity modes ω_n , and by substituting $N_n^2 2\pi/\tau$ for $d\omega$. The field $\hat{\mathbf{A}}^{(+)}(0,t)$ now includes radiation reflected from cavity walls along with radiation reaction. To evaluate (2) for $\hat{\mathbf{A}}^{(+)}(0,t)$ we assume that the boundaries of the cavity are in the radiation zone so that those cavity modes nearly in resonance with the atom are approximately evenly separated in frequency. The cavity mode most nearly in resonance with the atom will be denoted n_0 with frequency ω_{n_0} . Next, all cavity modes are thrown away in (6a) except M modes greater in frequency than ω_{n_0} and M modes lesser in frequency (with $M < n_0$). This approximation may be justified numerically (Figs. 3 and 4) or analytically (Appendix B). The field is

without complication to all of the Fourier components of $\hat{\mathbf{\Pi}}$ (except those near ω_1).

The analysis above is exactly true only in the limit of large n_0 (and small M), where the modes become evenly spaced in frequency. In general, the peaks of the kernel K do not remain narrow like a δ function, but with each recurrence, at integer multiples of τ , become broader. This “spreading” is equivalent to the spreading of the wave packet due to unequal spacings of cavity modes—the leading edge of the wave packet does not remain sharp as in Fig. 2. Elsewhere,¹⁰ we have shown how to predict the long-term evolution of kernels of this sort and, equivalently, of the wave packet. In the examples discussed here, the effects of spreading are insignificant.

The radiation-reaction term of (9) has a coefficient half that of the other terms, because as t' approaches t the integral (8) is over only half of the δ -function-like kernel K . This is reminiscent of the well-known result that vacuum fields are only half as effective in stimulating transitions as external fields.¹¹ The atom's own field returning from the boundaries behaves as an external field, but with an important difference: it stimulates only the transition that gave rise to it. It cannot, for example, stimulate a transition of the atom from the initial excited state $|e\rangle$ to a state of higher energy. Nor can it stimulate a transition to a state of lower energy other than the ground state of the transition that gave rise to the field. This is a generalization of the principle^{12,13} that in quantum electrodynamics there are no “lower-state beats”.

Now we can modify Eq. (5) for the rate of decay of the atom $[1/(\hbar\omega_a)]d\hat{H}_a/dt$:

$$\begin{aligned} \frac{d}{dt} \hat{\sigma}_{ee} = & -\frac{A_{eg}}{2} \hat{\sigma}_{ee}(t) - A_{eg} \hat{\sigma}_{eg}(t) \\ & \times \sum_{j=1}^{[t/\tau]} \hat{\sigma}_{ge}(t-j\tau) \exp(-i\omega_{n_0}j\tau) + \text{H.a.} \quad (10) \end{aligned}$$

Consider the m th kink, the discontinuity in $d\hat{\sigma}_{ee}/dt$ that occurs at $t=m\tau$. The angle of the m th kink is, for small ε ,

$$\begin{aligned} \frac{d}{dt}\hat{\sigma}_{ee}(m\tau+\varepsilon) - \frac{d}{dt}\hat{\sigma}_{ee}(m\tau-\varepsilon) \\ = -A_{eg}\hat{\sigma}_{eg}(m\tau)\hat{\sigma}_{ge}(m\tau+\varepsilon-m\tau) \\ \times \exp(-\omega_{n_0}m\tau) + \text{H.a.} \quad (11) \end{aligned}$$

We now apply this formula to the first nine kinks of Fig. 4(a), the first two Rabi oscillations. In the case of inhibited spontaneous emission the atom is only slightly perturbed by the vacuum fields and by the cavity fields. The atom remains nearly in its initial excited state, so we may use zeroth-order solutions of the $\hat{\sigma}$'s (Appendix A) to get

$$\frac{d}{dt}\hat{\sigma}_{ee}(t+\varepsilon) - \frac{d}{dt}\hat{\sigma}_{ee}(t-\varepsilon) = -2A_{eg}\hat{\sigma}_{ee}(0)\cos(\Delta t), \quad (12)$$

where t is the time of the m th kink $m\tau$. One can pursue this argument to derive the curve of Fig. 4(a), a Rabi oscillation of frequency $\Delta=\omega_{n_0}-\omega_a$.

In the example above [Fig. 4(a)] the walls of the cavity were perfect conductors. Light emitted at time $t-m\tau$ reflected off the boundaries m times to reach the atom at time t . After m reflections the light was out of phase with the oscillator (in its zeroth order solution) by $m\Delta$. Thus the $m\Delta$ has a geometrical origin indicating that the oscillator does not complete an integer number of cycles in the time it takes light to travel to boundaries and return. The examples of Figs. 1–4 illustrate the process by which the atom communicates with the boundaries at intervals of length τ .

V. RABI OSCILLATIONS IN THE KINKLESS LIMIT

In the limit in which the Rabi period is long compared to τ the Rabi oscillations lose their kinky character, the summation in Eq. (9) may be treated as an integral, and in the rotating-wave approximation (RWA), the equations of motion admit an exact solution. For example, the period of a Rabi oscillation of a typical one electron atom in resonance with a low-frequency cavity mode is of the order 1000τ . This is the limit in which we expect the multimode theory to reduce to the single-mode theory.

When the detuning is very large as in the example of Fig. 3 the kinks in the Rabi oscillation are unavoidable: when the detuning multiplied by 4.5 equals the frequency separation of cavity modes then there are always very nearly 4.5 kinks per Rabi period (for a typical atom). Such large detunings are properly treated as a special case (Sec. IV).

Let us repeat the derivation of $\hat{\mathbf{A}}^{(+)}$, but with fewer approximations and more general (semiclassical) boundary conditions. In Sec IV we showed that the field at the atom is a sum of terms representing fields radiated at earlier times $t-m\tau$. With each such term there was a phase factor of geometrical origin. We capitalize on this interpretation by introducing more complicated (semiclassical)

boundary conditions—due to dynamical as well as geometrical factors. For example, with each reflection from the boundary the field may suffer an energy loss and a phase shift of $-\Delta_1$. If, for each reflection, there is a fractional decrease in field energy of $2\Gamma\tau$ then after m reflections the phase factor in (9) must be multiplied by $(1-m\Gamma\tau)\exp(-i\Delta_1\tau m)$, for small Γ , or more generally $\exp[-(\Gamma+i\Delta_1)\tau m]$. It follows from (8) that

$$\begin{aligned} \hat{\mathbf{A}}^{(+)}(0,t) = -\frac{2e}{3mc^2} \frac{d}{dt} \hat{\mathbf{\Pi}}^{(+)}(t) \\ - \frac{4e}{3mc^2} \frac{d}{dt} \left[\sum_{m=1}^{\lfloor t/\tau \rfloor} \hat{\mathbf{\Pi}}^{(+)}(t-m\tau) \right. \\ \left. \times \exp(-i\tilde{\omega}m\tau) \right], \quad (13) \end{aligned}$$

where $\tilde{\omega} = -i\Gamma + \Delta_1 + \omega_a + \Delta$ and $\Delta = \omega_{n_0} - \omega_a$. In the limit in which the sum may be treated as an integral the radiation-reaction term may be treated as though it has the same coefficient as the other terms. The result is

$$\hat{\mathbf{A}}^{(+)}(0,t) = -\frac{1}{\tau} \frac{4e}{3mc^2} \frac{d}{dt} \int_0^t dt' \hat{\mathbf{\Pi}}^{(+)}(t') \exp[i\tilde{\omega}(t'-t)]. \quad (14)$$

It follows that

$$\begin{aligned} \frac{d}{dt} \hat{\mathbf{A}}^{(+)} + i(\omega_a + \Delta + \Delta_1 - i\Gamma) \hat{\mathbf{A}}^{(+)} \\ = -\frac{1}{\tau} \frac{4e}{3mc^2} \frac{d}{dt} \hat{\mathbf{\Pi}}^{(+)}. \quad (15) \end{aligned}$$

This equation for the time dependence of $\hat{\mathbf{A}}^{(+)}$ no longer follows from the Hamiltonian, Eq. (A1). However, the evolution of the atomic variables is still governed by (A1). In the RWA, the two required equations are

$$\frac{d}{dt} \hat{\mathbf{p}}_2^{(+)} + i\omega_a \hat{\mathbf{p}}_2^{(+)} = -i \frac{e}{\hbar mc} |p_{eg}|^2 \hat{W} \hat{\mathbf{A}}^{(+)} \quad (16)$$

and

$$\frac{d}{dt} \hat{W} = -i \frac{e}{\hbar mc} \hat{\mathbf{p}}_2^{(-)} \cdot \hat{\mathbf{A}}^{(+)} - i \frac{e}{\hbar mc} \hat{\mathbf{A}}^{(-)} \cdot \hat{\mathbf{p}}_2^{(+)}, \quad (17)$$

where $\hat{\mathbf{p}}_2^{(+)}$ is $\mathbf{p}_{ge}\hat{\sigma}_{ge}$ and \hat{W} is the inversion $\hat{\sigma}_{ee} - \hat{\sigma}_{gg}$. In the two-level atom, RWA $\hat{\mathbf{p}}_2^{(+)}$ takes the place of $\hat{\mathbf{p}}^{(+)}$.

Three equations (15), (16), and (17) strongly resemble the equations of motion of the single-mode Jaynes-Cummings model.¹⁴ To investigate the correspondence, we make two simplifications: we assume no damping, and we solve for $d\hat{\mathbf{A}}/dt$ in (15). The $d\hat{\mathbf{A}}/dt$ term on the right-hand side of (15) arises from the $\hat{\mathbf{A}} \cdot \hat{\mathbf{A}}$ part of the interaction Hamiltonian. It results in an insignificant frequency shift which can be incorporated into Δ and an insignificant shift in the coefficient of the atomic variable, which we neglect. From these three equations it can be shown that in the absence of damping the following quantities are constants of motion:

$$\hat{C}_1 = \frac{1 + \hat{W}}{2} + \frac{3c\tau}{4\hbar\omega_a} \hat{\mathbf{A}}^{(-)} \cdot \hat{\mathbf{A}}^{(+)}, \quad (18)$$

and

$$\begin{aligned} \hat{C}_2 = & \hat{H}_a - \frac{e}{mc} (\hat{\mathbf{A}}^{(-)} \cdot \hat{\mathbf{p}}_2^{(+)} + \hat{\mathbf{p}}_2^{(-)} \cdot \hat{\mathbf{A}}^{(+)}) \\ & + \hbar\omega_{n_0} \frac{3c\tau}{4\hbar\omega_a} \hat{\mathbf{A}}^{(-)} \cdot \hat{\mathbf{A}}^{(+)} . \end{aligned} \quad (19)$$

The first quantity \hat{C}_1 is called the excitation number. The second quantity \hat{C}_2 serves as an effective Hamiltonian if a certain commutation relation is postulated between $\hat{\mathbf{A}}^{(+)}$ and $\hat{\mathbf{A}}^{(-)}$. Because all vectors are in the direction \mathbf{p}_{eg} , we can suppress the vector character of $\hat{\mathbf{A}}$. If we were to set $[\hat{\mathbf{A}}^{(+)}, \hat{\mathbf{A}}^{(-)}] = 4\hbar\omega_a/(3c\tau)$ then \hat{C}_2 would be identical to the RWA Jaynes-Cummings Hamiltonian, and as a result the single-mode and multimode theories would be formally identical. (However, $[\hat{\mathbf{A}}^{(+)}, \hat{\mathbf{A}}^{(-)}] = 4\hbar\omega_a/(3c\tau)$ does not follow from the multimode equations.)

The solution of this set of equations is well known.¹⁴ The result is that $\hat{H}_a = \hbar\omega_a(\hat{W} + 1)/2$ undergoes Rabi oscillations of frequency $(\Delta^2 + \Omega_0^2)^{1/2}$ when the expectation value on initial state $|e\rangle$ is taken. Here Ω_0 equals $2(A_{eg}/\tau)^{1/2}$.

To understand these results and to compare them with the single-mode model we must first reexamine the RWA. The consequence of making the RWA is the neglect of the Bloch-Siegert shift, a frequency shift of order Ω_0^2/ω_a .

In Appendix B it is shown that the equations that result from discarding all cavity modes but the one nearly in resonance with the atom yield a Rabi frequency $[\Delta^2 + (\omega_a + \Delta)\Omega_0^2/\omega_a]^{1/2}$. It is easily verified that this differs from the Rabi frequency derived above only by a term of the same magnitude as the Bloch-Siegert shift.

Unlike the atom's excited-state population $\langle e | \hat{\sigma}_{ee} | e \rangle$, which oscillates with period $T_R = 2\pi/\Omega_0$ when the atom is in resonance with a cavity mode, the transition operator $\hat{\sigma}_{eg}(t)$ oscillates with a period $2T_R$, on resonance. In the multimode theory [Fig. 3(a)] this has a clear physical consequence in the angles of the kinks of Fig. 3(a). The oscillatory behavior of Fig. 3(a) has a period T_R , whereas the kinky behavior has a period $2T_R$. This may be easily understood by using the approximation solution $\hat{\sigma}_{eg}(0)\cos(\Omega_0 t/2)\exp(i\omega_{n_0} t)$ for $\hat{\sigma}_{eg}(t)$ when the atom is in resonance with a cavity mode. This solution neglects a term containing $\hat{\mathbf{A}}^{(-)}(0)$ which is of no importance here. When this is substituted into Eq. (11) for the angles of the kinks, Eq. (11) properly predicts the behavior of Fig. 3(a). The angles of the kinks are maximum near $t=0$, T_R , and $2T_R$, the angles approach zero in between these times, and the angles are opposite in sign at T_R and $2T_R$. Consequently, we have used solutions of equations formally identical to the single-mode equations to study multimode behavior. We will pursue this strategy systematically in Sec. VII.

It may be argued that solutions of equations identical to the single-mode equations [Eqs. (15), (16), and (17)] should be consistent with the single-mode commutation relation $[\hat{\mathbf{A}}^{(+)}, \hat{\mathbf{A}}^{(-)}]$. On the other hand, these equations are limiting forms of the multimode equations, where the commutator is a divergent c number. To

resolve this disagreement, and in general to answer questions about commutators, we cannot discard the term containing $\hat{a}_k(0)$ in the solution of $\hat{a}_k(t)$, Eq. (A5). Let us suppose that we have quantized the orthonormal cavity modes g_n so that $\hat{\mathbf{A}}^{(+)}$ is written $\sum \mathbf{A}_n \hat{a}_n$. Without discarding the operators $\hat{a}_n(0)$, the right-hand side of (15) must have the following operator added to it: $\hat{\mathbf{L}} = i \sum (\omega_{n_0} - \omega_n) \mathbf{A}_n \hat{a}_n(0) \exp(-i\omega_n t)$. The operator $\hat{\mathbf{L}}$ greatly complicates the equations and is sometimes treated as a Langevin operator. Because we have taken the radiation-reaction point of view and have normally ordered the equations of motion and the Hamiltonian, and because the initial state $|e\rangle$ is always a vacuum state, we are able to neglect $\hat{\mathbf{L}}$ in our analysis of multimode corrections in Sec. VII.

The transitions of interest to us here are the Rydberg-to-Rydberg transitions of one-electron atoms, particularly transitions from a state of principal quantum number n to the $n-1$ state. For such a two-level atom it is useful to calculate the actual size of the cavity enhancement. Let us assume that the atom is in resonance with a cavity mode of low frequency, say the tenth cavity mode as in Figs. 1–4. In the cavity the first correction to the zeroth-order time evolution of the atom $\exp(-i\omega_a t)$ is the frequency shift $\Omega_0^{n,n-1} = 2(A_{n,n-1}/\tau)^{1/2}$. It is found that $\Omega_0^{n,n-1}/\omega_a$ is of order $(\alpha^3/n^2)^{1/2}/10$. In free space the first correction to the zeroth-order solutions is the Einstein A -coefficient $A_{n,n-1}$. In free space the ratio $A_{n,n-1}/\omega_a$ is of order $(\alpha^2/n^2)/10$. So the enhancement $\Omega_0^{n,n-1}/A_{n,n-1}$ is of the order $1000n$. The next set of corrections, due to the counter-rotating terms and the $\hat{\mathbf{A}} \cdot \hat{\mathbf{A}}$ term, are of order α^3 smaller than ω_a in the cavity. In free space the corresponding ratio is α^6 . These estimates are roughly independent of the initial angular momentum of the dipole.

VI. PULSED EXCITATION OF A RYDBERG ATOM

The analysis of Secs. I–V might be criticized on the grounds that it was assumed that the atom was instantly excited from the ground state at $t=0$. The result of this model is that the leading edge of the wave packet (Fig. 2) is singular, whereas physical solutions of Schrödinger's equation do not permit such singularities. The problem is

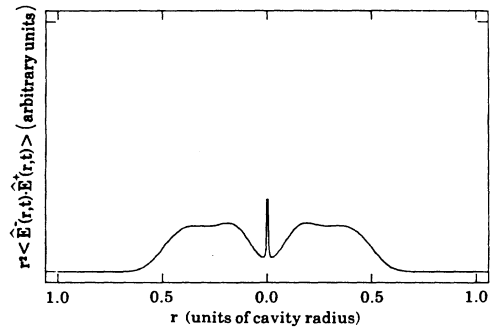


FIG. 5. Same as Fig. 2(a), but the atom has been prepared in the excited state at $t \simeq 0$ with a Gaussian-shaped laser pulse.

alleviated by slightly modifying the model to permit a pulsed excitation of the excited Rydberg state of the atom by a laser at optical frequencies. The microwave cavity can be given an aperture small enough to minimize microwave losses and large enough to admit the optical pulse. The result of such a model is shown in Fig. 5. The Schrödinger-picture equations of Appendix B were modified and solved numerically. The wave packet retains its relatively abrupt leading edge, but the singularities are gone.

In this model we want the two-level atom to be a Rydberg-to-Rydberg transition, ideally from a state of principal quantum number n to the $n-1$ state. In free space the most rapid transition is directly from the state n to the atom's ground state, an optical transition. The A coefficients have the ratio $A_{n,n-1}/A_{n,g} \simeq 0.5/n^2$. In the cavity, however, if the atom is in resonance with a mode of low frequency then the corresponding ratio is $\Omega_0^{n,n-1}/A_{n,g} \approx \alpha^{-3/2}/n$ or approximately $1000/n$. Finally we must worry about whether the n to $n-2$ transition is also in resonance with a cavity mode. Cases of this sort must be checked individually but this does not turn out to be a defect of the model.

VII. MULTIMODE CORRECTIONS TO THE SINGLE-MODE MODEL

The decay of two-level atom in a cavity may be characterized as the process by which an atom generates, as best it can, a single photon in a single-cavity mode, namely the mode nearest in frequency to the atom's transition frequency. It is worthwhile, then, to ask a question that cannot be answered by the single-mode models: how well does the atom succeed in placing a single photon in a single-cavity mode? A useful quantity in such a discussion is the dispersion in the field Hamiltonian $\Delta H_f = \langle \hat{H}_f^2 - \langle \hat{H}_f \rangle^2 \rangle^{1/2}$. After half a Rabi period $T_R/2 = \pi/\Omega_0$, the atom is in its ground state and $\Delta H_f/(\hbar 2\pi/\tau)$ has a clear physical meaning: it is the width Δn of the curve plotted in Fig. 1—the normalized probability distribution of photons in cavity modes $P_n = |b_n(t)|^2 / \sum_m |b_m(t)|^2$. In Fig. 6 we plot the time evolution of Δn .

Figure 6(a) shows a numerical solution of Δn over two Rabi periods. The dipole moment of the atom was chosen such that the Rabi period T_R equals 10τ . At $t = \tau, 2\tau$, and so on, Δn takes a sharp dip toward zero as the field distribution approaches that of the tenth cavity mode [Fig. 2(d)]. With time the packet spreads, the leading edge of the packet becomes less sharp, and the spikes become less apparent.

In the examples of Sec. III and Fig. 6(a) it is assumed that the atom is excited from the ground state to the excited state instantly at $t=0$. The example is instructive but unphysical. In Fig. 6(b) is plotted Δn in the case in which the atom is excited at $t \simeq 0$ with a smooth optical pulse (Sec. VI). The minimum of Δn in Fig. 6(b) is significantly smaller than the minimum of Δn in Fig. 6(a). The minimum of Δn in the sudden turn-on case [Fig. 6(a)] is dependent on the cutoff frequency ω_c of Eq. (2).

A difficulty arises in the calculation of ΔH_f because

$\langle \hat{H}_f \rangle$ generally diverges in nonrelativistic theory. As a result ΔH_f depends on the frequency cutoff ω_c of (2). However, if the model assumes a pulsed excitation of the atom [Fig. 6(b)], rather than a sudden turn on, then after half a Rabi period $T_R/2$, when the atom is in its ground state, $\langle \hat{H}_f \rangle$ is finite and ΔH_f independent of ω_c . The calculation is most easily done in the Schrödinger picture (Appendix B). Discarding self-energy, the amplitude of the n th mode is given by (B7)

$$b_n(t) = i \frac{\Omega_0 N_n}{2} \exp(-i\omega_n t) \times \int_{-\infty}^{\infty} dt' \mathcal{R}(t, t') b_e(t') \exp(i\omega_n t'), \quad (20)$$

where $\mathcal{R}(t, t')$ is as defined in Eq. (2). The probability that the atom is in the excited state is $|b_e(t)|^2$. The probability that the photon is in the n th mode is $|b_n(t)|^2$ so that $\langle \hat{H}_f \rangle$ is $\sum_n |b_n(t)|^2 \hbar \omega_n$.

The divergences of $\langle \hat{H}_f \rangle$ are a result of the discontinuities of the \mathcal{R} function, which introduce a $1/\omega_n$ dependence in $b_n(t)$ for large n . The dependence is $1/(\omega_n)^{1/2}$ if the self-energy term is not discarded. These divergences have a clear wave packet interpretation. When the spatial dependence of $\hat{A}^{(+)}$ is kept [Eq. (6)] the \mathcal{R} function of Eq. (20) [multiplied by $b_e(t)$] becomes the envelope of the wave packet. The discontinuity in the \mathcal{R} at $t'=0$ turns into the sharp leading edge of the wave packet due to the sudden turn-on of the atom. The discontinuity in the \mathcal{R} at $t'=t$ becomes the sharp edge of the wave packet at the

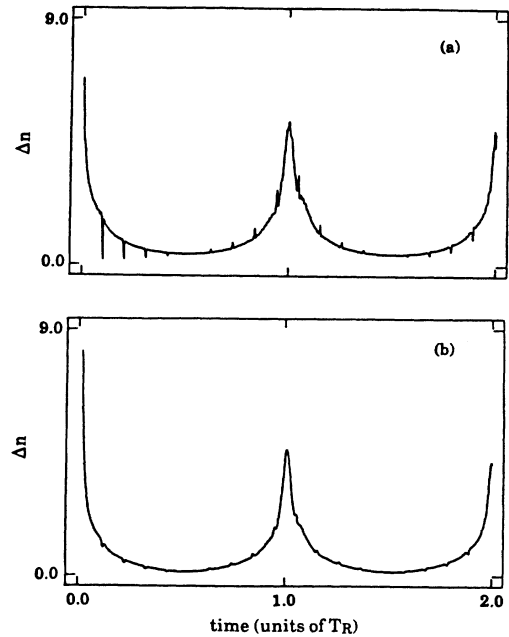


FIG. 6. Width (rms) of the normalized probability distribution P_n of photons in the cavity as the atom undergoes Rabi oscillations of period T_R . The atom is in resonance with the tenth cavity mode. (a) is the sudden turn-on case. In (b) the atom has been excited at $t \simeq 0$ with a laser pulse as in Fig. 5.

atom. In Fig. 2 is plotted the absolute square of the time derivative of $\hat{\mathbf{A}}^{(+)}$. It is apparent that the discontinuities in $\hat{\mathbf{A}}$ have become δ -function-like singularities. If the atom is turned on smoothly with a pulse at $t \simeq 0$ (Sec. VI) then the leading edge of the wave packet becomes differentiable (Fig. 5) and one source of divergence in $\langle \hat{H}_f \rangle$ is removed. It still diverges logarithmically due to the sharp edge of the wave packet at the atom. This is because we have made the dipole approximation and have assumed the atom to be a point particle. If the atom (or the electron) is given a finite size then $\langle \hat{H}_f \rangle$ is finite. The divergences, then, are due to the fact that it takes an infinite amount of energy to make wave functions with discontinuities.

We assume now that the atom is excited with a pulse at $t \simeq 0$ and that the atom is in resonance with a cavity mode so that the atom is in the ground state after half a Rabi period: $b_e(T_R/2) = 0$. (The \mathcal{R} function now must be modified so that it equals 1 for $t < 0$.) With these conditions, the \mathcal{R} function no longer introduces discontinuities into the integrand of (20), and ΔH_f is independent of ω_c . Because b_n is the Fourier transform of a smooth curve given by $b_e(t)$ (for $t < T_R/2$) we can immediately write down a time-energy Fourier relation,

$$\Delta H_f(T_R/2)\Delta t(T_R/2) \simeq \hbar, \quad (21)$$

where Δt is the standard deviation width (in time) of the curve determined by $|b_e(t)|^2$. If we divide $\Delta H_f(T_R/2)$ by the energy separation in modes $2\pi\hbar/\tau$ to get dispersion in modes Δn and multiply Δt by $2\pi/\tau$ to get $\Delta\Phi$ then we have at $t = T_R/2$ a number-phase relation $\Delta\Phi\Delta n \simeq 1$. A numerical calculation of Δt and of ΔH_f at $t = T_R/2$ verifies (21). The phase $\Delta\Phi$ to good approximation is found to be $\pi/2$ times the number of round trips the wave pack-

et makes in $T_R/2$.

By contrast, the single-mode Jaynes-Cummings theory yields the expected result that ΔH_f is zero at $t = T_R/2$.

To clarify the differences between the multimode and single-mode models we will show how to calculate expectation values of the multimode field Hamiltonian, its time derivatives, and its dispersion ΔH_f using the methods of Sec. V. To begin, it is convenient to rewrite Eq. (8) for $\hat{\mathbf{A}}^{(+)}(0, t)$ in terms of new variables:

$$\hat{\mathbf{A}}^{(+)}(0, t) = \sum_n \hat{a}_n \mathbf{A}_n, \quad (22a)$$

where \hat{a}_n satisfies

$$\frac{d}{dt} \hat{a}_n + i\omega_n \hat{a}_n = \frac{ie}{\hbar mc} \mathbf{A}_n \cdot \hat{\mathbf{p}}_2^{(+)} = \frac{i\Omega_0}{2} N_n \hat{\sigma}_{ge}(t), \quad (22b)$$

and where \mathbf{A}_n is $i\hbar mc \Omega_0 N_n \mathbf{p}_{eg} / (2e |\mathbf{p}|^2)$. The field Hamiltonian may be calculated in the usual way¹¹ by writing the electric field as a sum of the orthonormal cavity modes \mathbf{g}_n [Eq. (7)]. It follows that the RWA, normally ordered H_f is $\sum_n \hbar\omega_n \hat{a}_n^\dagger \hat{a}_n$, which we write

$$\hat{H}_f = \hat{H}_{f0} + \hat{H}_{f1} = \hbar\omega_{n_0} \sum_n \hat{a}_n^\dagger \hat{a}_n + \sum_n \hbar(\omega_n - \omega_{n_0}) \hat{a}_n^\dagger \hat{a}_n. \quad (23)$$

The second term on the right-hand side of (23), which we call \hat{H}_{f1} , is zero if all modes are discarded except the resonance mode of frequency ω_{n_0} . Consequently we expect \hat{H}_{f1} to be the multimode correction to the single-mode Jaynes-Cummings Hamiltonian. This is easily verified by substituting the formal solution of (22b) into (23). For \hat{H}_{f0} we find,

$$\hbar\omega_{n_0} \sum_n \hat{a}_n^\dagger \hat{a}_n = - \left[\frac{\Omega_0}{2} \right]^2 \hbar\omega_{n_0} \int_0^t \int_0^t dt' dt'' \hat{\sigma}_{eg}(t') K(t'' - t') \hat{\sigma}_{ge}(t'') \exp[i\omega_{n_0}(t'' - t')], \quad (24)$$

where the kernel K is given by (8b). The limiting process of Sec. V may be applied to (24). It is found that \hat{H}_{f0} becomes $\hbar\omega_{n_0} 3c\tau \hat{\mathbf{A}}^{(-)} \cdot \hat{\mathbf{A}}^{(+)} / (4\hbar\omega_a)$, exactly the fourth term of (19), the Jaynes-Cummings field Hamiltonian. The correction term \hat{H}_{f1} is calculated similarly, except that the kernel K in (24) is replaced with $-i\partial K/\partial t''$. The result is that to good approximation the expectation value of \hat{H}_{f1} equals the expectation value of $-\hbar\Delta 3c\tau \hat{\mathbf{A}}^{(-)} \cdot \hat{\mathbf{A}}^{(+)} / (4\hbar\omega_a)$, where $\Delta = \omega_{n_0} - \omega_a$. In physical terms this correction simply means that, in units of energy, the center of the photon probability distribution P_n (Fig. 1) is at the transition energy of the atom $\hbar\omega_a$, rather than the energy of the resonance mode $\hbar\omega_{n_0}$.

We have seen, then, that the single-mode Jaynes-Cummings model incorrectly predicts the expectation value of H_f . The limiting process described above may also be used to calculate the expectation values of the time derivatives of the Hamiltonian, with the result that the

Jaynes-Cummings model also incorrectly predicts the time derivatives. It may be verified that the limiting process described above correctly predicts that the multimode Hamiltonian $\hat{H}_a + \hat{H}_{\text{int}} + \hat{H}_{f0} + \hat{H}_{f1}$ is a constant of motion, and not $\hat{H}_a + \hat{H}_{\text{int}} + \hat{H}_{f0}$. Nevertheless, Eqs. (15), (16), and (17) are the correct limiting forms of the equations of motion and may be solved by the standard single-mode techniques to yield the quantities that appear in the multimode corrections described above.

We turn now to ΔH_f . Assuming that the atom is in resonance with a mode of frequency ω_{n_0} , ΔH_f^2 equals the expectation value of $\hbar \sum (\omega_n - \omega_{n_0})^2 \hat{a}_n^\dagger \hat{a}_n$ plus terms containing \hat{H}_{f0} that sum to zero when the atom is in its ground state. So, again it is found that the multimode correction is characterized by the presence of a power of $(\omega_n - \omega_{n_0})$. In this case, because it is the second power of $(\omega_n - \omega_{n_0})$, the correction may be calculated from (24) by replacing the kernel K with $-\partial^2 K/\partial t''^2$. Again we find

that the correction is easily written in terms of $\hat{\mathbf{p}}_2^{(+)}$, $\hat{\mathbf{A}}^{(+)}$, and so on, quantities that may be obtained by solving Eqs. (15), (16), and (17). The result is that the time-energy relation (21) is verified. The agreement is not quantitative because the relation (21) depends sensitively on the nature of the excitation of the atom, the details of which we neglect here.

VIII. CONCLUSION

The central analytical results of the paper followed from Eq. (13), in which the field at the atom $\hat{\mathbf{A}}^{(+)}(0,t)$ is written in terms of the acceleration of the electron $d(\hat{\mathbf{N}}/m)/dt$ at time t (the radiation-reaction field), and at earlier times $t-m\tau$ (radiated fields returning from the boundary). The wave packet interpretation of this formula allowed damping to be introduced in a natural way, and motivated a limiting process that yielded equations of motion formally identical to the single-mode Heisenberg-picture equations of motion. The same limiting process successfully yielded multimode corrections to the single-mode model, including a number-phase relation $\Delta n \Delta \Phi \approx 1$, describing how well the atom succeeds in placing a single photon in a single cavity mode.

Throughout we have attempted to characterize the physical behavior of the system in terms of the photon wave packet radiated by the atom: the sharp kinks in the Rabi oscillations were attributed to wave packets returning from the boundaries; the divergences in the field Hamiltonian were traced to discontinuities in the wave packet; the phase $\Delta \Phi$ was found to equal the number of round trips the wave packet makes in the lifetime of the atom multiplied by $\pi/2$. Resonance was characterized in terms of the relative phase of the dipole and of the fields returning from the boundary: a dipole is in resonance with the cavity if it completes an integer number of cycles in the time it takes the wave packet to reach the boundary and return to the dipole.

ACKNOWLEDGMENT

We would like to acknowledge the support of the Joint Services Optics Program.

APPENDIX A: HEISENBERG-PICTURE FORMALISM

We have chosen to work in the Heisenberg picture¹⁵ because it yields a far clearer physical picture than the Schrödinger picture. Furthermore, multilevel atoms are handled very naturally in the Heisenberg picture. Both of these virtues are apparent in Eq. (13) which relates the field at the atom $\hat{\mathbf{A}}^{(+)}(0,t)$ to the acceleration of the electron $d^2\hat{\mathbf{r}}/dt^2$. Keeping all the atomic levels in the Heisen-

berg approach permits a useful simplification (A8) and identification of the self-energy term (A6). The Schrödinger-picture equations specialize to the two-level atom at the beginning and as a result give somewhat different answers than the Heisenberg equations.

For convenience we start with a normal ordered Hamiltonian

$$\hat{H} = \hat{H}_a - \frac{e}{mc} \hat{\mathbf{p}} \cdot \hat{\mathbf{A}}^{(+)}(0,t) - \frac{e}{mc} \hat{\mathbf{A}}^{(-)}(0,t) \cdot \hat{\mathbf{p}} + \frac{e^2}{2mc^2} (\hat{\mathbf{A}} \cdot \hat{\mathbf{A}}^{(+)} + \hat{\mathbf{A}}^{(-)} \cdot \hat{\mathbf{A}}) + \hat{H}_f, \quad (\text{A1})$$

where \hat{H}_f is the free-field Hamiltonian and where $\hat{\mathbf{A}}^{(+)}$ is the $r \rightarrow 0$ limit of the positive frequency vector potential:

$$\hat{\mathbf{A}}^{(+)}(r,t) = \sum_k \mathbf{A}_k \hat{a}_k(t) \exp(i\mathbf{k} \cdot \mathbf{r}). \quad (\text{A2})$$

The field has been second quantized, $[\hat{a}_k, \hat{a}_k^\dagger] = 1$, but not the atom. The atomic variables are Heisenberg operators. They will be written as matrices, using as basis vectors the complete set of eigenstates of the atomic Hamiltonian. These matrices in turn are written as linear combinations of the transition operators $\hat{\sigma}_{ij}$. At $t=0$, the transition operator $\hat{\sigma}_{ij}$ is a matrix with a value of 1 at (row, column) = (i,j) and a value of 0 everywhere else. From that $t=0$ value of $\hat{\sigma}$ it follows that $\hat{\sigma}$ satisfies at any time the commutation relation

$$[\hat{\sigma}_{\alpha\beta}, \hat{\sigma}_{ij}] = \delta_{\beta i} \hat{\sigma}_{\alpha j} - \delta_{\alpha j} \hat{\sigma}_{i\beta}. \quad (\text{A3})$$

Any atomic Heisenberg operator may then be written as a linear combination of $\hat{\sigma}$'s. For example, the atomic Hamiltonian is

$$\hat{H}_a = \sum_{ij} \hat{\sigma}_{ij} \left\langle i \left| \frac{\mathbf{p} \cdot \mathbf{p}}{2m} + V(r) \right| j \right\rangle = \sum_i \hat{\sigma}_{ii} \hbar \omega_i, \quad (\text{A4})$$

where the sum runs over all eigenstates of the atomic Hamiltonian $|i\rangle$ and $|j\rangle$, and $\hbar \omega_i$ is the energy of the i th eigenstate.

The equation of motion for the field amplitude \hat{a}_k may be formally integrated to give

$$\hat{a}_k(t) = \exp(-i\omega_k t) \times \left[\hat{a}_k(0) + \int_0^t dt' \exp(i\omega_k t') e \hat{\mathbf{N}}(t') \cdot \mathbf{A}_k / mc \right]. \quad (\text{A5})$$

Setting $\mathbf{r}=0$ in (A2), summing over polarizations, and integrating over angular variables, we find

$$\hat{\mathbf{A}}^{(+)}(0,t) = -\frac{2e}{3\pi mc^2} \frac{d}{dt} \int_0^{\omega_c} d\omega \exp(-i\omega t) \int_{-\infty}^{\infty} dt' \mathcal{P}(t,t') \hat{\mathbf{N}}(t') \exp(i\omega t') + \frac{2e}{3\pi mc^2} \omega_c \hat{\mathbf{N}}(t). \quad (\text{A6})$$

The second term on the right-hand side of (A6) can be identified as the self-energy of the electron. Henceforth this term will be discarded.

In Sec. IV we showed how to evaluate the integral in (A6). The result in free space is that $\hat{\mathbf{A}}^{(+)}$ is to a good approximation proportional to the positive frequency part of $\hat{\mathbf{P}}$:

$$\hat{\mathbf{A}}^{(+)}(0,t) = -\frac{2e}{3mc^2} \frac{d}{dt} \left[\hat{\mathbf{p}}^{(+)} - \frac{e}{c} \hat{\mathbf{A}}^{(+)}(0,t) \right]. \quad (\text{A7})$$

The positive frequency atomic operator $\hat{\mathbf{p}}^{(+)}$ was defined in Sec. II. A consequence of the definition of $\hat{\mathbf{p}}^{(+)}$ is that differentiation commutes with the positive frequency operation:

$$\frac{d}{dt} \hat{\mathbf{p}}^{(+)} = \left[\frac{d}{dt} \hat{\mathbf{p}} \right]^{(+)} = \left[\sum_{ij} \hat{\sigma}_{ij} i\omega_{ij} \mathbf{p}_{ij} \right]^{(+)}. \quad (\text{A8})$$

where ω_{ij} equals $\omega_i - \omega_j$.

Because the vacuum fields perturb the atom so weakly, the zeroth-order solutions of the atomic variables are extremely useful. To get the zeroth-order solutions the equations are solved as though there were no vacuum field. In the case of a two-level atom the zeroth-order solution of $\hat{\mathbf{p}}^{(+)}$ is

$$\hat{\mathbf{p}}^{(+)} = \hat{\sigma}_{ge}(0) \mathbf{p}_{ge} \exp(i\omega_{ge}t), \quad (\text{A9})$$

where $|g\rangle$ is the ground state, $|e\rangle$ the excited state, and \mathbf{p}_{ge} the matrix element of $\hbar\nabla/i$.

$$\mathbf{A}_{(+)}(0,t) = i \frac{2e}{3\pi mc^2} \int_0^{\omega_c} d\omega \exp(-i\omega t) \omega \int_{-\infty}^{\infty} dt' \mathcal{R}(t,t') \left[\mathbf{p}_{ge} b_e - \frac{e}{c} \mathbf{A}_{(+)} \right] \exp(i\omega t'). \quad (\text{B4})$$

where $\mathbf{A}_{(+)}$ is $\sum_k \mathbf{A}_k b_k(t)$. Schrödinger's equation implies the following equation of motion for $\mathbf{p}_{ge} b_e(t)$:

$$\frac{d}{dt} \mathbf{p}_{ge} b_e + i\omega_a \mathbf{p}_{ge} b_e = i \frac{e}{\hbar mc} |p_{eg}|^2 \mathbf{A}_{(+)}. \quad (\text{B5})$$

Equations (B4) and (B5) correspond to the Heisenberg-picture Eqs. (2) and (16). The cavity modifications are unchanged from the Heisenberg approach of Sec. II. Equation (B4) inserted into (B5) yields

$$\begin{aligned} & \frac{d}{dt} b_e + i\omega_a b_e \\ &= -\frac{A_{eg}}{\tau\omega_a} \sum_n N_n^2 \omega_n \int_0^t dt' b_e(t') \exp[i\omega_n(t'-t)]. \end{aligned} \quad (\text{B6})$$

APPENDIX B: SCHRÖDINGER-PICTURE FORMALISM

To write the equations of motion in the Schrödinger picture, we assume a wave function of the form

$$|\Psi\rangle = b_e(t) |e\rangle + \sum_k b_k(t) |1_{k,g}\rangle, \quad (\text{B1})$$

where $|1_{k,g}\rangle$ is a state with one photon in the k th mode, and the atom in the ground state. Schrödinger's equation, restricted to this set of states, has been extensively studied, beginning with the work of Wigner and Weisskopf.¹⁶ Emphasis has been on studying causality in quantum electrodynamics.¹⁷ Here we wish to establish connection with the Heisenberg equations and to apply boundary conditions. The Schrödinger-picture equations have the advantage of being easy to solve numerically and analytically. In Sec. VII, use of the Schrödinger-picture equations permitted a straightforward and quantitative calculation of the ΔH_f . Furthermore, they help to justify the less familiar Heisenberg radiation-reaction approach. In particular the Heisenberg-picture rotating-wave approximation will be better justified in view of the results below. The Hamiltonian is (A1), although it need not be normal ordered. The connection with the Heisenberg picture follows from

$$\begin{aligned} \langle \Psi(0) | \hat{\sigma}_{ee}(t) | \Psi(0) \rangle &= \langle \Psi(t) | \hat{\sigma}_{ee}(0) | \Psi(t) \rangle \\ &= |b_e(t)|^2, \end{aligned} \quad (\text{B2})$$

and

$$\begin{aligned} \langle \Psi(0) | \hat{\mathbf{E}}^{(-)}(r,t) \cdot \hat{\mathbf{E}}^{(+)}(r,t) | \Psi(0) \rangle \\ = \left| \sum_k \frac{\omega_k}{c} \mathbf{A}_k b_k(t) \exp(i\mathbf{k}\cdot\mathbf{r}) \right|^2. \end{aligned} \quad (\text{B3})$$

Just as in the derivation of (2) and (A6), Schrödinger's equation implies

We use the many-level atom Heisenberg theory, specifically Eqs. (A6), (A7), and (A8), to apply boundary conditions and to argue that the self-energy of the electron is discarded by simply replacing $N_n^2 \omega_n$ in (B6) with $N_n^2 \omega_a$. With this modification (B6) is equivalent to

$$\frac{d}{dt} b_e + i\omega_a b_e = i \sum_n C_n b_n, \quad (\text{B7})$$

and

$$\frac{d}{dt} b_n + i\omega_n b_n = iC_n b_e, \quad (\text{B8})$$

where $C_n = N_n \Omega_0 / 2$. If we had kept the self-energy term of (A6), then we would have found $C_n = (\omega_n / \omega_a)^{1/2} N_n \Omega_0 / 2$. Equations of this sort appear frequently in semiclassical models as well and have been

widely studied.¹⁸ In particular Kyrölä¹⁹ has investigated the single-mode limit of the multimode equations.

We are now prepared to justify our choice of $N_n^2 2\pi/\tau$ as the substitution for $d\omega$ in (2). The modified equations must satisfy two requirements. First of all, before the wave packet reaches the boundaries, the cavity-modified equations must give the same results as the free-space equations. The fact that $N_n=1$ (very nearly) for all but the smallest n guarantees this since then the substitution for $d\omega$ is $\omega_{n+1}-\omega_n$. (Atoms in resonance with the first cavity mode are a complication we ignore in this discussion.) The second requirement is that the amplitudes $b_n(t)$ behave as quantum-mechanical amplitudes. From Eqs. (B7) and (B8) it is apparent that the time evolution of the amplitudes $b_e(t), b_n(t)$ is governed by a Hermitian matrix so that $|b_e|^2 + \sum |b_n(t)|^2 = 1$. This is the equivalent of (19). Next, to get $\langle H_f \rangle$ we integrate (B3) over the cavity volume and divide by 2π , but first rewrit-

ing the right-hand side as a sum of cavity modes g_n [Eq. (7)] as in (6). It is verified that $N_n^2 2\pi/\tau$ is the unique substitution for $d\omega$ such that the Hamiltonian of (B7) and (B8) is Hermitian and $\langle H_f \rangle$ is $\sum_n \hbar\omega_n |b_n(t)|^2$.

The single-mode approximation may be motivated by a simple argument. We see that the right-hand side of (B6) is a sum of the Fourier components of the slowly varying quantity $b_e(t)\exp(i\omega_a t)$ (multiplied by an unimportant \mathcal{R} function). The slowly varying quantity oscillates at the Rabi frequency, which is typically much less than the frequency separation of cavity modes. The Fourier transform of $b_e\exp(i\omega_a t)$, then is a curve that falls to zero rapidly for ω of the order $2\pi/\tau$ and larger. Consequently, the elements of the sum on the right-hand side of (B6) are all much smaller than the $n=n_0$ element. Throwing away all but $n=n_0$ term yields a simple equation that predicts a Rabi frequency of $[\Delta^2 + (\omega_a + \Delta)\Omega_0^2/\omega_a]^{1/2}$. However, this answer is not unique.

- ¹E. T. Jaynes and F. W. Cummings, IEEE Proc. 51, 89 (1963).
²P. Goy, J. M. Raimond, M. Gross, and S. Haroche, Phys. Rev. Lett. 50, 1903 (1983).
³R. G. Hulet, E. S. Hilfer, and D. Kleppner, Phys. Rev. Lett. 55, 2137 (1985).
⁴G. S. Agarwal, R. K. Bullough, and G. P. Hildred, Opt. Commun. 59, 23 (1986).
⁵P. Dobiasch and H. Walther, Ann. Phys. (Paris) 10, 825 (1985).
⁶G. S. Agarwal, Phys. Rev. Lett. 53, 1732 (1984).
⁷G. Gabrielse and H. Dehmelt, Phys. Rev. Lett. 55, 67 (1985).
⁸L. S. Brown, K. Helmerson, and J. Tan, Phys. Rev. A 34, 2638 (1986); L. S. Brown and G. Gabrielse, Rev. Mod. Phys. 58, 233 (1986).
⁹M. Born and E. Wolf, *Principles of Optics* (Pergamon, New York, 1980) 6th ed., p. 82.
¹⁰J. Parker and C. R. Stroud, Jr., Phys. Rev. Lett. 56, 716 (1986).
¹¹L. I. Schiff, *Quantum Mechanics* (McGraw-Hill, New York, 1968) 3rd ed., pp. 490–533.
¹²I. C. Khoo and J. H. Eberly, Phys. Rev. A 14, 2174 (1976).

- ¹³R. M. Herman, H. Grotch, R. Kornblith, and J. H. Eberly, Phys. Rev. A 11, 1389 (1975).
¹⁴L. Allen and J. H. Eberly, *Optical Resonance and Two-Level Atoms* (Wiley, New York, 1975), pp. 157–162.
¹⁵P. W. Milonni, Phys. Rep. 25c, 3 (1976).
¹⁶V. F. Weisskopf and E. Wigner, Z. Phys. 63, 54 (1930).
¹⁷E. Fermi, Rev. Mod. Phys. 4, 91 (1932); G. Breit, *ibid.* 5, 91 (1933); J. Hamilton, Proc. R. Soc. London, Ser. A 62, 12 (1949); P. W. Milonni and P. L. Knight, Phys. Rev. A 10, 1096 (1974).
¹⁸M. Bixon and J. Jortner, J. Chem. Phys. 48, 7 (1968); G. C. Stey and R. W. Gibberd, Physica (Utrecht) 60, 7 (1972); R. Lefebvre and J. Savolainen, J. Chem. Phys. 60, 2509 (1972); W. M. Gelbart, D. F. Heller, and M. L. Elert, Chem. Phys. 7, 116 (1975); B. W. Shore and J. H. Eberly, Opt. Commun. 24, 83 (1978); J. J. Yeh, C. M. Bowden, and J. H. Eberly, J. Chem. Phys. 76, 5936 (1982); P. W. Milonni, J. R. Ackerhalt, H. W. Galbraith, and Mei-Li Shih, Phys. Rev. A 28, 32 (1983).
¹⁹E. Kyrölä, J. Opt. Soc. Am. B 1, 737 (1984).